Journal of Molecular Spectroscopy **195,** 299–307 (1999)
Article ID jmsp.1999.7833, available online at http://www.idealibrary.com on IDEAL®

Fourier Transform Emission Spectroscopy of the $[12.8]^2\Phi$–$a^2\Phi$ System of TiCl

R. S. Ram and P. F. Bernath[1]

Department of Chemistry, University of Arizona, Tucson, Arizona 85721

Received November 20, 1998

High-resolution emission spectra of TiCl have been recorded in the 10 000–18 000 cm^{-1} region using a Fourier transform spectrometer. The molecules were excited in a microwave discharge through a flowing mixture of $TiCl_4$ and helium. TiCl bands observed in the 11 000–13 500 cm^{-1} region have been assigned to a new $[12.8]^2\Phi$–$a^2\Phi$ electronic transition with the 0–0 bands of $^2\Phi_{5/2}$–$^2\Phi_{5/2}$ and $^2\Phi_{7/2}$–$^2\Phi_{7/2}$ subbands at 12 733.7 and 12 791.5 cm^{-1}, respectively. A rotational analysis of several bands has been obtained, and spectroscopic constants have been extracted. This assignment is supported by the available theoretical calculations and is also consistent with the near infrared measurements of a doublet–doublet transition of ZrCl [J. G. Phillips, S. P. Davis, and D. C. Galehouse, *Astrophys. J. Suppl. Ser.* **43,** 417–434) (1980)].

INTRODUCTION

In recent years, the study of transition metal diatomic halides has attracted considerable attention (*1–3*). Because of high cosmic abundances of transition metal elements, these molecules are potentially of astrophysical importance. Recently we studied the electronic spectra of TiF (*1*), TiCl (*2*), and ZrCl (*3*) and have shown that these molecules have $^4\Phi$ ground states. Our work on these transition metal halides started when we initially observed the $G^4\Phi$–$X^4\Phi$ transition of TiF in the visible region using laser excitation and Fourier transform emission spectroscopy (*1*). Our assignment of a $^4\Phi$ ground state for TiF was consistent with the recent *ab initio* calculations by Harrison (*4*). For TiCl, three new electronic transitions, assigned as $C^4\Delta$–$X^4\Phi$, $G^4\Phi$–$C^4\Delta$, and $G^4\Phi$–$X^4\Phi$, were identified in the 3000–12 000 cm^{-1} region (*2*). For ZrCl, the $C^4\Delta$–$X^4\Phi$ transition was observed in the 3800–4300 cm^{-1} region, again consistent with a $^4\Phi$ ground state (*3*). The ground state assignments of TiCl and ZrCl have also been confirmed by recent calculations by Boldyrev and Simons (*5*) and Focsa *et al.* (*6*) (for TiCl) and by Focsa *et al.* (*7*) (for ZrCl). In addition to the ground state, these authors have also predicted the spectroscopic properties of some low-lying doublet and quartet excited states of TiCl (*5, 6*) and ZrCl (*7*).

The emission spectrum of TiCl was first observed by Fowler (*8*) in 1907 using an arc source. Several complex bands were observed in the 400–420 nm region, which were reinvestigated by several workers in emission as well as in absorption (*9–16*). These studies focused mainly on the vibrational assignment of these bands. Moore and Parker (*9*) assigned them to a doublet–doublet transition, while Rao (*10*) and Shenyavskaya *et al.* (*11*) assigned them as a $^4\Pi$–$^4\Sigma^-$ transition. Similar assignments were also proposed by Chatalic *et al.* (*12*) and Diebner and Kay (*13*). The rotational analysis of a few strong bands in the 400–420 nm region was obtained by Lanini (*14*) and Phillips and Davis (*16*). Lanini (*14*) assigned these bands to a $^2\Phi$–$^2\Delta$ transition, while Phillips and Davis (*16*) assigned them into four $\Delta\Omega = 1$ doublet–doublet electronic transitions. In our TiCl (*2*) and ZrCl (*3*) papers we suggested that this transition was either $^4\Delta$–$X^4\Phi$ or $^4\Gamma$–$X^4\Phi$. The very recent work of Imajo *et al.* (*17*) has confirmed the $^4\Gamma$–$X^4\Phi$ assignment.

During the study of TiCl spectra in the 3000–12 000 cm^{-1} region (*2*), we noted that several bands remained unclassified due to their complexity and weaker intensity. To obtain an assignment and to search for other transitions to higher wavenumbers, we have recorded again the emission spectra of TiCl in the 10 000–18 000 cm^{-1} region. The new bands observed in the 11 000–13 500 cm^{-1} region have been assigned to a new doublet–doublet transition analogous to that observed for ZrCl by Phillips *et al.* (*18*) in the 8700–10 300 cm^{-1} region. Rotational analysis of this transition will be presented in this paper and its electronic assignment will be discussed in the light of the recent theoretical calculations.

EXPERIMENTAL DETAILS

The experimental details and observation procedures for TiCl spectra have been described in our previous paper (*2*). In summary, the TiCl molecules were excited in a microwave discharge through a flowing mixture of helium and a trace of $TiCl_4$ vapor. The spectra were recorded with the 1-m Fourier transform spectrometer of the National Solar Observatory at Kitt Peak. The spectra in the 10 000–18 000 cm^{-1} interval were recorded using a visible beam splitter and Si photodiode detectors. A total of five scans were coadded in about 30 min of integration at a resolution of 0.02 cm^{-1}.

[1] Also Department of Chemistry, University of Waterloo, Waterloo, Ontario, Canada N2L 3G1.

0022-2852/99 $30.00

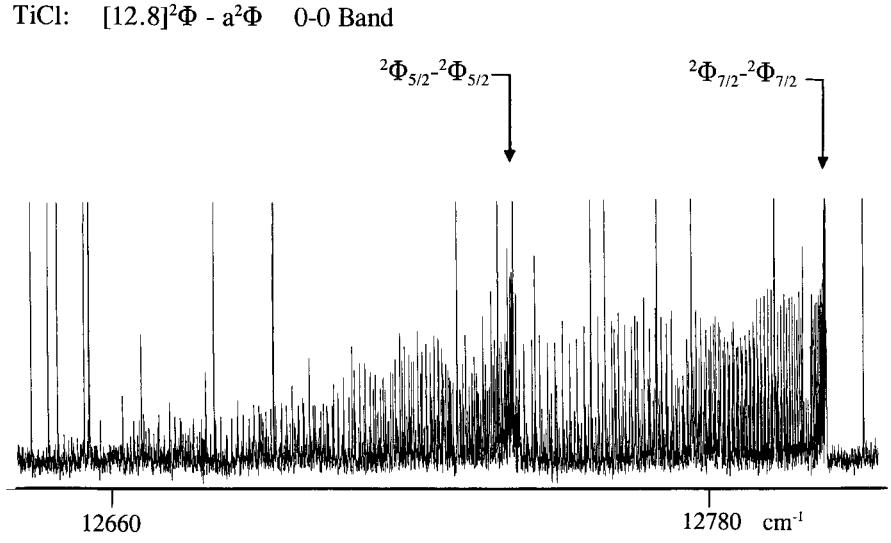

FIG. 1. A compressed portion of the 0–0 band of the $[12.8]^2\Phi$–$a^2\Phi$ system of TiCl.

The spectral line positions were determined using a data reduction program called PC-DECOMP developed by J. Brault. The peak positions were determined by fitting a Voigt lineshape function to each line. Because this spectrum lacked strong impurity CO or other atomic or molecular lines necessary for wavenumber calibration, we decided to use strong atomic lines as transfer standards. For this purpose we chose the previously recorded TiCl spectrum (*2*) in which both HCl 1–0 vibration–rotation lines and the atomic lines were present. The atomic lines were first calibrated using the HCl lines (*19*) and then the calibration was transferred to the present spectrum of TiCl. The molecular lines of TiCl have a typical width of 0.03 cm^{-1} and appear with a maximum signal-to-noise ratio of 12:1, so that the best linepositions are expected to be accurate to about ± 0.002 cm^{-1}.

RESULTS AND DISCUSSION

The new emission bands of TiCl are located in the 11 000–13 500 cm^{-1} region and consist of four groups in the 12 200–12 400 cm^{-1}, 12 600–12 800 cm^{-1}, 13 000–13 200 cm^{-1}, and 13 400–13 600 cm^{-1} intervals. A careful inspection of the spectrum indicates that each group consists of two subbands and can be assigned as the 0–1, 0–0, 1–0, and 2–0 bands of a new doublet–doublet transition. The bands in the 13 400–13 600 cm^{-1} interval are weaker than the bands in the other three groups. In addition to these bands, there are several very weak bands near 11 618, 12 057, 12 390, 12 450, 12 561, and 12 844 cm^{-1} which still remain unassigned. Of these bands, a band near 11 618 cm^{-1} is probably the 2–0 band of the $G^4\Phi$–$X^4\Phi$ transition. Inspection of rotational structure of this band indicates that it is strongly perturbed and a rotational analysis could not be obtained.

Of the new bands, the two bands observed in the 12 600–12 800 cm^{-1} interval are the strongest in intensity and have been assigned as the 0–0 band of the two subbands of a doublet–doublet transition. This transition is most probably the band system analogous to the near infrared transition of ZrCl reported previously by Phillips *et al.* (*18*). A part of the spectrum of this band is presented in Fig. 1, where the proposed assignments have been marked.

The structure of each band consists of single R and P branches consistent with a $\Delta\Omega = 0$ transition between states having high Ω values. An expanded part of the rotational structure of the $[12.8]^2\Phi_{7/2}$–$a^2\Phi_{7/2}$, 0–0 band is presented in Fig. 2, where the lines of the most abundant $Ti^{35}Cl$ have been marked. The lines of the minor isotopomer $Ti^{37}Cl$ were also identified in our spectra, but the molecular constants have been determined only for the most abundant $^{48}Ti^{35}Cl$ isotopomer. Ti has five isotopes, ^{46}Ti (8%), ^{47}Ti (7.3%), ^{48}Ti (73.8%), ^{49}Ti (5.5%), and ^{50}Ti (5.4%), but the lines involving the weaker titanium isotopes were not identified in our spectra. With the help of the available theoretical calculations on TiCl (*6*) and ZrCl (*7*), we have assigned this system as $[12.8]^2\Phi$–$a^2\Phi$ transition.

No cross transitions with $\Delta\Sigma \neq 0$ were observed in our spectra so that the spin–orbit intervals could not be determined directly. The rotational constants for the two spin components of the observed states were determined by fitting the lines of both subbands separately using a simple term energy expression (Eq. [1]), although the observed electronic states most likely obey Hund's case (a) coupling.

$$F_v(J) = T_v + B_v J(J+1) - D_v[J(J+1)]^2 + H_v[J(J+1)]^3. \quad [1]$$

The rotational lines were given weights based on resolution, extent of blending, and effect of perturbations. Perturbed lines

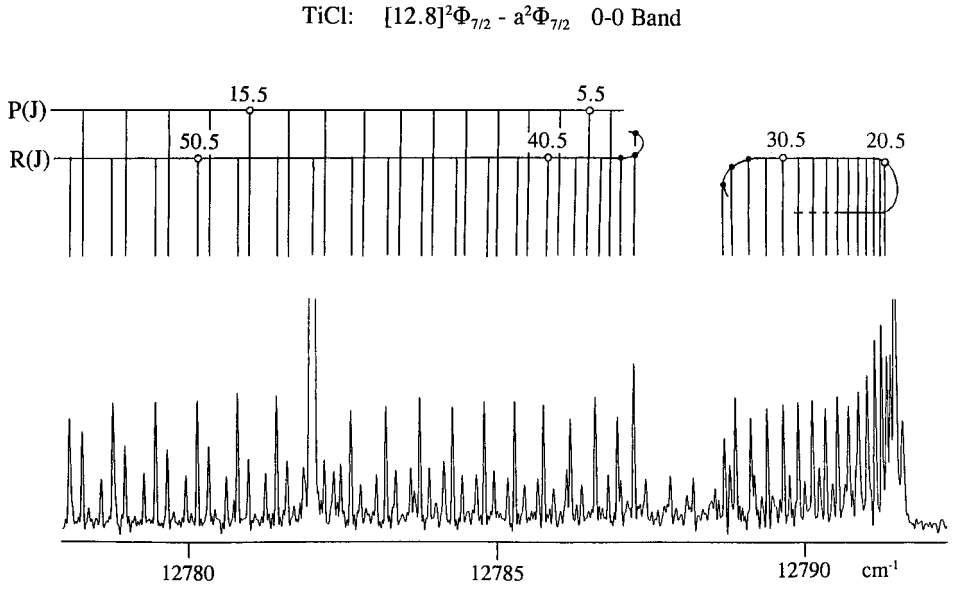

FIG. 2. An expanded portion of the 0–0 band of the $[12.8]^2\Phi_{7/2}$–$a^2\Phi_{7/2}$ subband of $Ti^{35}Cl$ near the *R* head. The *R* branch shows a strong perturbation near $J = 35.5$. The unmarked lines are due to the minor isotopomer $Ti^{37}Cl$.

were not included in the fit, although the combination differences for the unperturbed levels, for example for $v = 0$ and 1 of $[12.8]^2\Phi_{7/2}$, were included in the fit. The inclusion of the higher order constant H_v for some vibrational levels is a reflection of interactions with other electronic states. The observed line positions for the different subbands are provided in Table 1 and the molecular constants for the $a^2\Phi$ and $[12.8]^2\Phi$ states are provided in Table 2.

A rotational analysis of the 0–0 and 1–0 bands of the $[12.8]^2\Phi_{7/2}$–$a^2\Phi_{7/2}$ subband indicates the presence of a strong local perturbation in the $v = 0$ vibrational level of the lower state near $J'' = 35.5$. The perturbation observed in the *R* branch of the 0–0 band can clearly be noticed in Fig. 2. The high *J* lines of the 0–0 band of the $[12.8]^2\Phi_{5/2}$–$a^2\Phi_{5/2}$ subband are also affected by perturbations. The *P*-branch lines of this subband appear to split into two components near $J'' = 40.5$. This splitting increases rapidly with increasing *J*, and it becomes difficult to follow lines beyond $J'' = 43.5$ in one Ω component and $J'' = 54.5$ in the other Ω component. This splitting is most probably due to perturbations which affect the two Ω components differently. Although the band heads of the 0–1 and 2–1 bands of the $[12.8]^2\Phi_{5/2}$–$a^2\Phi_{5/2}$ subband are clearly present at 12 321.7 and 13 113.3 cm^{-1}, the rotational lines were not identified because of their weak intensity and overlapping from other bands as well as perturbations. The structure of only the 0–0 and 1–0 bands of the $[12.8]^2\Phi_{5/2}$–$a^2\Phi_{5/2}$ subband could be rotationally analyzed. In contrast, the rotational structure of eight bands, 0–1, 1–2, 0–0, 1–1, 1–0, 2–1, 3–1, and 4–2, of the $[12.8]^2\Phi_{7/2}$–$a^2\Phi_{7/2}$ subband has been identified and analyzed.

Although the TiCl bands in the visible and near ultraviolet regions have been known for decades, the identity of the ground state has always been in question. The present observation strongly suggests that the $a^2\Phi$ lower state is not the ground state of TiCl, consistent with our recent assignment of the $X^4\Phi$ ground state (*2*). These observations are also supported by recent theoretical calculations on TiCl (*6*), which predict the first doublet excited state, $a^2\Phi$, at about 8800 cm^{-1} above the ground $X^4\Phi$ state. The local perturbation observed in the $a^2\Phi_{7/2}$ spin component is caused by a doublet or quartet state located in the vicinity. In particular, a $^2\Delta$ and a $^4\Delta$ state have been predicted in the region of the $a^2\Phi$ state, but other states are possible. Boldyrev and Simons (*5*) did not predict the spectroscopic properties of the low-lying $^2\Phi$ state, and they implicitly assumed that a $^2\Delta$ state is the lowest state in the doublet manifold of TiCl (*5*). However, the work of Focsa *et al.* on TiCl (*6*) and ZrCl (*7*) predict a $^2\Phi$ state to be lowest in the doublet manifold of TiCl and ZrCl, based on ligand field theory. At this stage we are unable to confirm definitely whether the observed lowest doublet state is a $^2\Delta$ or $^2\Phi$ state, but the absence of Ω doubling in the observed bands indicates that the doublet states of $\Omega > 1$ are involved in this transition of TiCl and ZrCl (*18*). In this paper we have preferred to label the lower state as the $a^2\Phi$ state. It is possible, but less likely, that our bands belong to a $^2\Delta$–$^2\Delta$ transition. Note that the assignment of the 7/2 and 5/2 spin components was based only on the relative size of the effective *B* values in the a $^2\Phi$ state and is also not secure.

The electron configurations of the observed states of TiCl are expected to be similar to those of TiF (*4*) and TiH (*20*). A correlation diagram of the energy levels of TiCl, TiF, TiH, and Ti^+ is provided in our previous paper (*2*) where the $^4\Phi$ assignment of the ground state of TiCl has been justified. The lowest a^4F $(3d^24s^1)$ term of Ti^+ correlates to the $X^4\Phi$, $A^4\Sigma^-$, $B^4\Pi$,

TABLE 1

Observed Line Positions (in cm^{-1}) for the $[12.8]^2\Phi$–$a^2\Phi$ Transition of TiCl

J	R(J)	O-C	P(J)	O-C	R(J)	O-C	P(J)	O-C	R(J)	O-C	P(J)	O-C
	$[12.8]^2\Phi_{7/2}$ - $a^2\Phi_{7/2}$ 0-1				$[12.8]^2\Phi_{7/2}$ - $a^2\Phi_{7/2}$ 0-0				$[12.8]^2\Phi_{7/2}$ - $a^2\Phi_{7/2}$ 1-0			
2.5									13193.079	-4		
3.5									13193.326	-8	13190.722	-10
4.5									13193.558	-5	13190.306	-4
5.5					12790.285	14			13193.762	-9	13189.864	-4
6.5					12790.479	7			13193.954	-4	13189.408	3
7.5					12790.660	6	12785.407	-12	13194.117	-6	13188.915	-4
8.5					12790.819	2	12784.917	-10	13194.271	4	13188.416	3
9.5			12361.473	0	12790.961	0	12784.409	-7	13194.397	7	13187.889	3
10.5					12791.088	4	12783.880	-7			13187.338	1
11.5			12360.443	-1	12791.194	5	12783.333	-4			13186.769	3
12.5			12359.902	-2	12791.280	6	12782.765	-4			13186.182	6
13.5			12359.346	0	12791.339	-2	12782.179	-2			13185.571	8
14.5			12358.763	-9			12781.575	2			13184.939	11
15.5			12358.170	-11	12791.412	-3	12780.952	6			13184.287	14
16.5			12357.567	-6	12791.412 *	-11	12780.310 *	9	13194.682 *	30	13183.612 *	15
17.5			12356.945	-2			12779.646 *	10	13194.626 *	23	13182.915 *	16
18.5			12356.310	5			12778.964 *	13	13194.560 *	26	13182.198 *	18
19.5			12355.635	-10	12791.339 *	9	12778.266 *	18	13194.469 *	27	13181.461 *	21
20.5			12354.965	-4	12791.280 *	20	12777.546 *	21	13194.354 *	24	13180.703 *	25
21.5			12354.279	4	12791.194 *	23	12776.806 *	24	13194.220 *	24	13179.920 *	25
22.5	12368.600	-7	12353.566	2	12791.088 *	26	12776.049 *	28	13194.072 *	31	13179.121 *	31
23.5	12368.535	3	12352.840	3	12790.961 *	26	12775.273 *	34	13193.895 *	31	13178.299 *	35
24.5	12368.437	-3	12352.093	1	12790.819 *	32	12774.480 *	41	13193.705 *	40	13177.454 *	37
25.5	12368.335	4	12351.333	3	12790.660 *	39	12773.664 *	44	13193.489 *	44	13176.590 *	42
26.5	12368.208	4	12350.556	5	12790.479 *	45	12772.832 *	51	13193.251 *	47	13175.717 *	58
27.5	12368.060	0	12349.765	11	12790.285 *	55	12771.980 *	57	13192.995 *	55	13174.800 *	52
28.5	12367.899	0	12348.932	-9	12790.073 *	69	12771.115 *	69	13192.721 *	65	13173.883 *	69
29.5	12367.726	5	12348.114	4	12789.841 *	82	12770.230 *	81	13192.429 *	80	13172.940 *	79
30.5	12367.525	0	12347.267	5	12789.596 *	100	12769.332 *	98	13192.116 *	94	13171.983 *	98
31.5	12367.314	3	12346.399	2	12789.335 *	122	12768.423 *	124	13191.788 *	116	13171.013 *	125
32.5	12367.084	3	12345.519	3	12789.068 *	157	12767.505 *	161	13191.458 *	158	13170.028 *	158
33.5	12366.835	2	12344.617	1	12788.818 *	230	12766.610 *	239	13191.134 *	227	13169.061 *	231
34.5	12366.566	-3	12343.697	-3	12788.639 *	393	12765.773 *	396	13190.883 *	392	13168.164 *	396
35.5	12366.287	1	12342.770	4	12787.175 *	-710	12763.665 *	-701	13189.349 *	-706	13165.978 *	-706
36.5	12365.975	-11	12341.820	4	12787.175 *	-330	12762.997 *	-337	13189.256 *	-340	13165.236 *	-343
37.5	12365.669	0	12340.855	7	12786.909 *	-196	12762.088 *	-196	13188.915 *	-200	13164.253 *	-200
38.5	12365.333	-3	12339.863	0	12786.549 *	-137	12761.081 *	-133	13188.475 *	-137	13163.168 *	-137
39.5	12364.984	1	12338.860	-2	12786.148 *	-99	12760.025 *	-100	13187.986 *	-101	13162.032 *	-103
40.5	12364.612	-3	12337.841	-2	12785.714 *	-75	12758.941 *	-75	13187.459 *	-82	13160.863 *	-80
41.5	12364.225	-3	12336.805	-1	12785.251 *	-60	12757.831 *	-58	13186.907 *	-64	13159.665 *	-65
42.5	12363.822	-2	12335.766	13	12784.764 *	-50	12756.694 *	-48	13186.328 *	-52	13158.446 *	-48
43.5	12363.402	-2	12334.680	-3	12784.256 *	-41	12755.537 *	-39	13185.722 *	-44	13157.192 *	-44
44.5	12362.965	-1	12333.595	-1	12783.727 *	-34	12754.359 *	-32	13185.094 *	-37	13155.920 *	-37
45.5	12362.499	-11	12332.491	0	12783.176 *	-29	12753.160 *	-27	13184.441 *	-31	13154.625 *	-30
46.5	12362.036	-2	12331.370	0	12782.607 *	-23	12751.940 *	-23	13183.760 *	-31	13153.306 *	-26
47.5	12361.543	-5	12330.228	-3			12750.696 *	-24	13183.066 *	-21	13151.963 *	-23
48.5			12329.076	-1	12781.406 *	-15	12749.444 *	-13	13182.345 *	-16	13150.600 *	-17
49.5	12360.515	-2	12327.905	1	12780.775 *	-13	12748.160 *	-15	13181.604 *	-8	13149.213 *	-14
50.5	12359.974	-1	12326.717	2	12780.126	-8	12746.866	-9	13180.830	-10	13147.803	-11
51.5	12359.413	-3	12325.508	-1	12779.457	-5	12745.548	-7	13180.038	-7	13146.371	-7
52.5	12358.846	5	12324.287	0	12778.768	-2	12744.210	-6	13179.225	-1	13144.918	-3
53.5	12358.236	-12	12323.049	2	12778.055	-4	12742.855	-3	13178.385	0	13143.436	-4
54.5	12357.632	-6	12321.782	-9	12777.324	-3	12741.477	-2	13177.515	-6	13141.935	-1
55.5	12357.010	-2	12320.533	15	12776.576	-1	12740.081	-1	13176.634	2	13140.412	2
56.5	12356.370	1	12319.237	8	12775.808	2	12738.663	-3			13138.863	3
57.5	12355.708	-1	12317.923	0	12775.019	3	12737.230	-1			13137.288	1
58.5	12355.034	3	12316.597	-4	12774.208	1	12735.778	1	13173.827	3	13135.700	10

TABLE 1—*Continued*

												P2
J	R(J)	O-C	P(J)	O-C	R(J)	O-C	P(J)	O-C	R(J)	O-C	P(J)	O-C
59.5	12354.341	4	12315.265	3	12773.381	3	12734.303	0	13172.846	5	13134.075	4
60.5	12353.627	0	12313.905	-2	12772.533	3	12732.805	-5	13171.837	4	13132.440	13
61.5	12352.907	7	12312.533	-3	12771.667	5	12731.297	0	13170.800	-1	13130.773	12
62.5	12352.158	1	12311.147	-1	12770.777	3	12729.767	1	13169.736	-7	13129.073	4
63.5	12351.399	3	12309.742	-3	12769.870	2	12728.222	7	13168.650	-12	13127.347	-7
64.5	12350.627	7	12308.321	-4	12768.946	5	12726.648	3			13125.610	-4
65.5	12349.846	18	12306.890	0	12767.999	4	12725.053	-3			13123.835	-15
66.5	12349.028	8	12305.437	-2	12767.032	3	12723.442	-6				
67.5	12348.194	-1	12303.965	-7	12766.044	1	12721.823	2				
68.5	12347.361	6	12302.480	-9	12765.046	8	12720.173	0				
69.5			12300.988	-4	12764.017	3	12718.509	2				
70.5			12299.479	0	12762.997	27	12716.822	0				
71.5			12297.951	0	12761.907	1	12715.119	2				
72.5					12760.823	1	12713.393	-1				
73.5					12759.720	1	12711.653	2				
74.5					12758.595	-2	12709.890	1				
75.5					12757.458	3	12708.110	3				
76.5					12756.291	-2	12706.309	2				
77.5					12755.112	0	12704.488	0				
78.5					12753.914	3	12702.635	-13				
79.5					12752.690	0	12700.786	-4				
80.5					12751.447	-2	12698.912	-1				
81.5					12750.187	-3	12697.017	1				
82.5					12748.910	0	12695.103	3				
83.5					12747.612	2	12693.152	-13				
84.5					12746.290	-2	12691.209	-2				
85.5					12744.951	-2	12689.245	8				
86.5					12743.589	-5	12687.254	10				
87.5					12742.217	1	12685.243	10				
88.5							12683.187	-15				
89.5							12681.140	-11				
	$[12.8]^2\Phi_{7/2}$ - $a^2\Phi_{7/2}$ 2-1				$[12.8]^2\Phi_{7/2}$ - $a^2\Phi_{7/2}$ 1-1				$[12.8]^2\Phi_{7/2}$ - $a^2\Phi_{7/2}$ 1-2			
7.5	13168.068	-6	13162.930	0								
8.5	13168.198	-4	13162.424	9								
9.5	13168.296	-10	13161.879	1								
10.5	13168.384	-4	13161.320	3			12764.410	-7				
11.5	13168.432	-14	13160.736	3			12763.871	-3				
12.5	13168.484	4	13160.124	-2	12771.772	6	12763.321	10			12341.232	-15
13.5	13168.484	-7	13159.500	4	12771.827	-7	12762.725	-4			12340.680	-9
14.5	13168.484	6	13158.846	4	12771.887	4					12340.113	-1
15.5	13168.432	-11	13158.168	3	12771.917	4	12761.502	-6			12339.521	0
16.5	13168.384	2	13157.468	3	12771.917	-7			12349.964	-3	12338.918	6
17.5	13168.296	-2	13156.743	3	12771.917	2	12760.209	-2	12349.994	3	12338.282	-4
18.5	13168.198	9	13155.995	3	12771.887	-1	12759.539	5	12349.994	-3	12337.639	-3
19.5	13168.068	13	13155.212	-8	12771.827	-14	12758.838	0	12349.994	9	12336.977	-5
20.5	13167.898	0	13154.421	-2	12771.772	-3	12758.130	7	12349.964	8	12336.301	-2
21.5	13167.714	-2	13153.601	-2	12771.691	1	12757.402	14	12349.910	0	12335.606	-3
22.5	13167.516	8	13152.758	1	12771.587	2	12756.638	3	12349.846	-1	12334.895	-1
23.5	13167.272	-3	13151.886	-2	12771.462	1	12755.868	6	12349.765	-1	12334.163	-4
24.5	13167.012	-5	13150.989	-3	12771.324	6			12349.667	-1	12333.425	5
25.5	13166.733	0	13150.064	-9			12754.259	1	12349.557	4	12332.662	6
26.5	13166.421	-2	13149.125	-3	12770.964	-9	12753.435	7	12349.419	-1	12331.877	2
27.5	13166.086	-1	13148.161	4	12770.777	6	12752.588	9	12349.272	2	12331.080	3
28.5	13165.721	-3	13147.159	-2	12770.550	-1	12751.711	2	12349.094	-9		
29.5	13165.334	-2	13146.136	-2	12770.306	-4	12750.823	2				
30.5	13164.917	-2	13145.083	-5	12770.055	5	12749.914	0	12348.712	-4	12328.585	6
31.5	13164.474	-2	13144.016	3	12769.770	0	12748.984	-3	12348.494	-2	12327.711	-2
32.5	13164.014	9	13142.907	-3	12769.471	0	12748.031	-10	12348.259	0	12326.834	6

TABLE 1—*Continued*

P3

J	R(J)	O-C	P(J)	O-C	R(J)	O-C	P(J)	O-C	R(J)	O-C	P(J)	O-C
33.5	13163.504	-1	13141.777	-4	12769.150	-2	12747.085	10	12348.008	4	12325.927	0
34.5	13162.978	1	13140.623	-1	12768.815	2	12746.090	1	12347.732	-1	12325.012	4
35.5	13162.420	-1	13139.439	0			12745.086	1	12347.444	1	12324.077	4
36.5	13161.837	0	13138.229	4	12768.067	-10	12744.059	-2	12347.137	1	12323.121	1
37.5	13161.224	3	13136.985	1	12767.676	-4	12743.013	-5	12346.818	6	12322.150	1
38.5	13160.581	4	13135.700	-13			12741.950	-4	12346.466	-3	12321.161	0
39.5	13159.905	3	13134.415	1	12766.809	-15	12740.869	-2	12346.112	3	12320.160	4
40.5	13159.199	3	13133.086	2	12766.367	1	12739.767	-2	12345.730	-2	12319.142	8
41.5	13158.449	-11	13131.730	6	12765.884	-5			12345.334	-2	12318.095	0
42.5	13157.697	5	13130.342	7	12765.386	-5	12737.500	-5	12344.921	-2	12317.036	-1
43.5	13156.893	2	13128.915	1	12764.874	1	12736.338	-6	12344.488	-4	12315.963	0
44.5	13156.061	2	13127.478	15	12764.338	3	12735.157	-5	12344.035	-9	12314.867	-3
45.5			13125.986	7	12763.772	-5	12733.959	-2	12343.575	-2	12313.759	-1
46.5	13154.292	-2	13124.471	9	12763.192	-7	12732.747	8	12343.089	-3	12312.631	-2
47.5	13153.358	-2	13122.907	-8	12762.597	-3	12731.493	-6	12342.590	1	12311.485	-3
48.5	13152.381	-11	13121.334	2	12761.978	-3	12730.236	-1	12342.069	1	12310.321	-4
49.5	13151.393	4	13119.713	-3	12761.339	-2	12728.954	-2	12341.524	-5	12309.140	-5
50.5	13150.344	-6	13118.082	15	12760.679	-1	12727.656	2	12340.962	-10	12307.945	-1
51.5	13149.269	-5	13116.380	-1			12726.330	-3	12340.397	2	12306.723	-7
52.5			13114.657	-5	12759.304	6	12724.997	5	12339.803	1		
53.5	13147.009	-2	13112.893	-12			12723.633	3	12339.192	3	12304.244	1
54.5	13145.814	-9	13111.103	-9	12757.831	-1	12722.259	11	12338.564	7	12302.981	8
55.5	13144.598	3	13109.273	-8	12757.074	6	12720.854	9			12301.701	17
56.5	13143.334	6			12756.291	9	12719.415	-8				
57.5	13142.036	16			12755.481	5	12717.983	4				
58.5					12754.651	2	12716.526	12				
59.5					12753.806	5	12715.039	9				
60.5					12752.924	-6	12713.536	12				
61.5					12752.042	3						
62.5					12751.118	-8	12710.453	2				
63.5					12750.187	-5	12708.885	2				
64.5							12707.297	3				
	$[12.8]^2\Phi_{7/2}$ - $a^2\Phi_{7/2}$ 3-1				**$[12.8]^2\Phi_{7/2}$ - $a^2\Phi_{7/2}$ 4-2**				**$[12.8]^2\Phi_{5/2}$ - $a^2\Phi_{5/2}$ 0-0**			
4.5									12732.328	5		
5.5									12732.541	-9		
6.5									12732.748	-11	12728.171	-3
7.5											12727.711	2
8.5											12727.231	4
9.5											12726.725	-1
10.5			13570.786	14					12733.421	8		
11.5			13570.160	-1					12733.534	3	12725.670	0
12.5			13569.520	-3					12733.634	3	12725.115	0
13.5									12733.715	3	12724.537	-5
14.5	13577.739	2	13568.171	-3					12733.774	-1	12723.952	1
15.5	13577.661	-2	13567.461	0					12733.829	8	12723.342	0
16.5	13577.563	0	13566.727	4			13536.670	-11	12733.853	5	12722.714	-1
17.5	13577.439	1	13565.966	5	13547.419	-6			12733.853	-5	12722.068	-2
18.5	13577.282	-8	13565.173	-1	13547.296	-11			12733.853	4	12721.406	0
19.5	13577.110	-5	13564.359	-2	13547.154	-11	13534.425	8	12733.829	6	12720.724	-2
20.5	13576.918	2	13563.537	14	13546.996	-4	13533.611	-4	12733.774	-4	12720.027	-1
21.5			13562.682	20	13546.813	4	13532.783	-6	12733.715	-1	12719.312	1
22.5	13576.436	-8	13561.770	-5	13546.596	0	13531.937	-2	12733.634	-3	12718.575	-3
23.5	13576.158	-13	13560.873	9	13546.359	0	13531.073	7	12733.534	-6	12717.826	-1
24.5			13559.917	-11	13546.096	-2	13530.175	5	12733.421	-5	12717.059	0
25.5			13558.968	-1	13545.820	6	13529.251	2	12733.291	-2	12716.275	0
26.5					13545.512	7	13528.292	-14	12733.143	-2	12715.473	0
27.5	13574.832	-3	13556.978	2	13545.175	3	13527.350	13	12732.979	0	12714.656	3
28.5	13574.447	6	13555.942	0	13544.821	6	13526.360	13	12732.805	9	12713.820	3

TABLE 1—*Continued*

P4

J	R(J)	O-C	P(J)	O-C	R(J)	O-C	P(J)	O-C	R(J)	O-C	P(J)	O-C
29.5	13574.028	5	13554.890	4	13544.438	3			12732.603	6	12712.970	4
30.5	13573.586	6	13553.788	-16	13544.031	0	13524.299	7	12732.388	7	12712.103	6
31.5	13573.114	0	13552.700	0	13543.602	-1	13523.239	9	12732.165	15	12711.228	15
32.5	13572.620	-3	13551.574	3	13543.153	3	13522.146	3	12731.905	4	12710.316	3
33.5	13572.107	-2			13542.670	-4	13521.034	0	12731.629	-9	12709.394	-3
34.5	13571.574	3					13519.904	4	12731.358	-2	12708.460	-7
35.5	13571.011	2	13548.037	-4			13518.745	3	12731.064	-3	12707.520	-1
36.5	13570.424	1	13546.813	-5	13541.101	1	13517.559	-1	12730.760	2	12706.560	-2
37.5	13569.815	0	13545.569	-2	13540.525	-2	13516.356	1	12730.435	-1	12705.589	2
38.5	13569.180	-1	13544.296	-4	13539.929	-1	13515.131	5	12730.102	3	12704.603	3
39.5									12729.773 *	24	12703.616 *	17
39.5	13568.527	1	13543.012	5	13539.314	5	13513.867	-6	12729.758	8	12703.597	-3
40.5	13567.843	-3	13541.691	2	13538.666	2	13512.588	-8	12729.422 *	35	12702.630 *	44
40.5									12729.380	-7	12702.578	-9
41.5	13567.146	3	13540.346	-3	13537.992	-3	13511.288	-7	12729.061 *	49	12701.612 *	51
41.5									12729.007	-4	12701.552	-9
42.5	13566.416	-1	13538.987	2	13537.301	0	13509.966	-3	12728.712 *	87	12700.607 *	83
42.5									12728.623	-2	12700.519	-5
43.5	13565.665	-1	13537.595	-3	13536.581	-2			12728.408 *	181	12699.645 *	170
43.5									12728.222	-4	12699.487	11
44.5	13564.894	0	13536.187	0	13535.836	-5			12727.831 *	13	12698.427 *	10
45.5	13564.094	-3	13534.757	3	13535.084	10	13505.842	-9	12727.426 *	26	12697.370 *	21
46.5	13563.277	1	13533.292	-5	13534.273	-10	13504.431	1	12727.023 *	52	12696.323 *	52
47.5	13562.432	-1	13531.822	4	13533.467	0			12726.595 *	60	12695.249 *	63
48.5	13561.558	-7	13530.315	0			13501.508	-8	12726.201 *	110	12694.195 *	102
49.5	13560.675	0	13528.788	-1			13500.015	-8	12725.794 *	154	12693.152 *	158
50.5	13559.762	1	13527.236	-4			13498.491	-15	12725.408 *	224	12692.102 *	213
51.5	13558.823	0	13525.671	3			13496.970	6	12725.053 *	331	12691.094 *	314
52.5			13524.070	-2			13495.380	-19	12724.714 *	457	12690.116 *	450
53.5	13556.879	3	13522.455	2			13493.822	13	12724.426 *	638	12689.183 *	632
54.5	13555.869	2	13520.810	-2			13492.201	6	12724.214 *	895	12688.311 *	877
55.5	13554.833	-1	13519.148	2			13490.566	10				
56.5			13517.465	8			13488.893	-1				
57.5												
58.5			13514.009	1								
59.5			13512.247	-1								
60.5			13510.460	-4								

J	R(J)	O-C	P(J)	O-C	J	R(J)	O-C	P(J)	O-C	J	R(J)	O-C	P(J)	O-C
						$[12.8]^2\Phi_{5/2}$ - $a^2\Phi_{5/2}$ 1-0								
7.5	13133.923	4	13128.719	10	24.5	13133.818	-2	13117.550	-1	40.5	13128.768 *	38	13102.115 *	26
8.5	13134.075	2	13128.213	1	25.5	13133.637	-1	13116.716	-3	40.5	13128.719	-11	13102.084	-5
9.5	13134.197	-11	13127.694	-1	26.5	13133.438	2	13115.875	7	41.5	13128.326 *	53	13101.033 *	48
10.5	13134.321	-1	13127.144	-14	27.5	13133.213	-2	13114.998	0	41.5	13128.271	-2	13100.975	-10
11.5	13134.415	-0	13126.587	-13	28.5	13132.974	-1	13114.115	6	42.5	13127.887 *	85	13099.951 *	84
12.5	13134.501	12	13126.030	7	29.5	13132.723	6	13113.201	-1	42.5	13127.798	-3	13099.860	-7
13.5	13134.544	1	13125.424	-2	30.5	13132.440	-0	13112.278	1	43.5	13127.478 *	160	13098.906 *	169
14.5	13134.582	6	13124.814	5	31.5	13132.162	16	13111.344	11	43.5			13098.738	2
15.5			13124.172	0	32.5	13131.834	1	13110.377	5	44.5			13097.604 *	10
16.5			13123.515	0	33.5	13131.488	-16	13109.381	-13	45.5			13096.454 *	15
17.5			13122.831	-7	34.5	13131.150	-6	13108.392	-6	46.5			13095.320 *	46
18.5	13134.501	-9	13122.140	-1	35.5	13130.793	1	13107.390	3	47.5			13094.160 *	62
19.5	13134.442	-2	13121.418	-7	36.5	13130.416	5	13106.355	-3	48.5				
20.5	13134.355	-4	13120.686	-4	37.5	13130.014	0	13105.311	-3	49.5			13091.863 *	143
21.5	13134.257	3	13119.931	-3	38.5	13129.607	6	13104.261	8	50.5			13090.732 *	213
22.5	13134.129	0	13119.159	0	39.5					51.5			13089.619 *	308
23.5	13133.979	-6	13118.376	11	39.5	13129.177	4	13103.184	6					

Note. Asterisks mark perturbed lines, see text for details.

TABLE 2
Molecular Constants (in cm^{-1}) for the $a^2\Phi$ and $[12.8]^2\Phi$ States of TiCl

	$[12.8]^2\Phi_{5/2}$		$[12.8]^2\Phi_{7/2}$				
Const.	v=0	v=1	v=0	v=1	v=2	v=3	v=4
T_v	12730.7474(14)	13131.7942(14)	12788.48923(77)	13192.03771(86)	13589.1239(18)	13998.7179(19)	14390.6171(24)
B_v	0.163800(14)	0.162837(14)	0.1636226(29)	0.1626398(41)	0.1608000(50)	0.1593556(51)	0.1594786(47)
$D_v \times 10^7$	1.133(56)	1.150(57)	1.1215(35)	1.230(17)	4.310(28)	-0.959(27)	1.553(12)
$H_v \times 10^{11}$	--	--	--	-0.542(26)	-1.507(55)	-2.160(48)	--

	$a^2\Phi_{5/2}$	$a^2\Phi_{7/2}$		
Const.	v=0	v=0	v=1	v=2
T_v	0.0	0.0	423.0585(13)	845.2719(15)
B_v	0.172926(15)	0.1732882(29)	0.1721356(35)	0.1712597(38)
$D_v \times 10^7$	1.604(88)	1.1091(36)	0.847(10)	1.2985(88)
$H_v \times 10^{11}$	-5.92(22)	--	-0.446(13)	--

Note. Values in parentheses are one standard deviation uncertainty in the last digits.

and $C^4\Delta$ states of TiCl, where the $X^4\Phi$ state is the ground state. The higher lying $A^4\Sigma^-$, $B^4\Pi$, and $C^4\Delta$ states of TiCl have been predicted near 1456, 2450, and 5650 cm^{-1}, respectively, by Focsa *et al.* (*6*). The first excited state b^4F ($3d^3$) of Ti^+ correlates with the $D^4\Delta$ (5300 cm^{-1}), $E^4\Pi$ (8770 cm^{-1}), $F^4\Sigma^-$ (9970 cm^{-1}), and $G^4\Phi$ (11 570 cm^{-1}) states according to the calculations of Focsa *et al.* (*6*). We have experimentally observed the $C^4\Delta$ and $G^4\Phi$ states of TiCl near 3300 and 10 900 cm^{-1}, respectively. The next higher excited a^2F ($3d^24s^1$) state of Ti^+ correlates with $^2\Phi$, $^2\Sigma^-$, $^2\Pi$, and $^2\Delta$ states which have been calculated near 8400, 9850, 10 200, and 10 420 cm^{-1}, respectively (*6*). Ligand field theory thus predicts that the doublets and quartets of the a^4F and a^2F terms of the Ti^+ $3d^24s^1$ configuration have the same energy ordering: Φ, Σ^-, Π, and Δ. A similar ordering of states has also been predicted for ZrCl (*7*). We have, therefore, labeled the $^2\Phi$ state as the $a^2\Phi$ state following the usual spectroscopic convention. A high quality *ab initio* calculation is needed to confirm our assignments.

Our analysis indicates that some excited state vibrational levels of the $[12.8]^2\Phi_{7/2}$ spin component are also affected by global perturbations (Table 2). For example, the constants of Table 2 provide $\Delta G_{1/2}$ = 403.5485(12) cm^{-1}, $\Delta G_{3/2}$ = 397.0862(20) cm^{-1}, $\Delta G_{5/2}$ = 409.5940(26) cm^{-1}, and $\Delta G_{7/2}$ = 391.8992(31) cm^{-1} for the $[12.8]^2\Phi_{7/2}$ spin component. The abnormal value of $\Delta G_{5/2}$ clearly indicates the effect of global interactions of the $v = 2$ and 3 vibrational levels with another state (or states). This can also be confirmed from the rotational constants of $v = 2$ and 3 vibrational levels which have abnormal magnitudes for B_v and D_v values. The constants of Table 2 have been used to determine the approximate values for the equilibrium constants, in spite of global interactions in both the lower and upper states. After deweighting the values for the perturbed levels, equilibrium vibrational constants ω_e = 423.9036(27) cm^{-1}, $\omega_e x_e$ = 0.4226(12) cm^{-1} for the $a^2\Phi_{7/2}$ and ω_e = 405.5595(51) cm^{-1}, $\omega_e x_e$ = 1.0055(11) cm^{-1} for the $[12.8]^2\Phi_{7/2}$ spin components have been obtained. The equilibrium vibrational constants could not be determined for the $a^2\Phi_{5/2}$ and $[12.8]^2\Phi_{5/2}$ spin components due to lack of sufficient data, although a $\Delta G_{1/2}$ = 401.0468(20) cm^{-1} has been obtained for the $[12.8]^2\Phi_{5/2}$ spin component. A similar treatment of the rotational constants of Table 2 provides B_e = 0.17377(12) cm^{-1}, α_e = 0.00103(8) cm^{-1} for $a^2\Phi_{7/2}$, B_e = 0.164155(52) cm^{-1}, α_e = 0.001039(24) cm^{-1} for the $[12.8]^2\Phi_{7/2}$, and B_e = 0.164282(17) cm^{-1}, α_e = 0.000963(20) cm^{-1} for $[12.8]^2\Phi_{5/2}$ spin components. The equilibrium rotational constants for the $a^2\Phi_{5/2}$ spin component could not be determined. These constants provide the bond lengths of r_0 = 2.19565(10) Å for $a^2\Phi_{5/2}$, r_e = 2.19031(75) Å for $a^2\Phi_{7/2}$, r_e = 2.25268(12) Å for $[12.8]^2\Phi_{5/2}$, and r_e = 2.2535(36) Å for the $[12.8]^2\Phi_{7/2}$ spin components.

CONCLUSIONS

We have recorded the emission spectrum of TiCl in the 10 000–18 000 cm^{-1} region using a Fourier transform spectrometer. A number of new bands observed in the 11 000–13 500 cm^{-1} region have been assigned to a new $[12.8]^2\Phi$–$a^2\Phi$ electronic transition with the 0–0 bands of the $^2\Phi_{5/2}$–$^2\Phi_{5/2}$ and $^2\Phi_{7/2}$–$^2\Phi_{7/2}$ subbands at 12 733.7 and 12 791.5 cm^{-1}, respectively. This transition is analogous to the near infrared transition of ZrCl reported by Phillips *et al.* (*18*). These observations are also supported by recent theoretical calculations on TiCl (*6*) and ZrCl (*7*), but more theoretical work is needed.

ACKNOWLEDGMENTS

We thank M. Dulick of the National Solar Observatory for assistance in obtaining the Spectra. The Kitt Peak National Observatory and the National Solar Observatory are operated by the Association of Universities for Research in Astronomy, Inc., under contract with the National Science Foundation. The

research described here was supported by funding from the NASA laboratory astrophysics program. Some support was also provided by the Natural Sciences and Engineering Research Council of Canada and the Petroleum Research Fund administered by the American Chemical Society.

REFERENCES

1. R. S. Ram, J. R. D. Peers, Y. Teng, A. G. Adam, A. Muntianu, P. F. Bernath, and S. P. Davis, *J. Mol. Spectrosc.* **184,** 186–201 (1997).
2. R. S. Ram and P. F. Bernath, *J. Mol. Spectrosc.* **186,** 113–130 (1997).
3. R. S. Ram and P. F. Bernath, *J. Mol. Spectrosc.* **186,** 335–348 (1997).
4. J. F. Harrison, private communication.
5. A. I. Boldyrev and J. Simons, *J. Mol. Spectrosc.* **188,** 138–141 (1998).
6. C. Focsa, M. Bencheikh, and L. G. M. Pettersson, *J. Phys. B: At. Mol. Phys.* **31,** 2857–2869 (1998).
7. C. Focsa, private communication.
8. A. Fowler, *Proc. Roy. Soc. A* **79,** 509 (1907).
9. K. R. More and A. H. Parker, *Phys. Rev.* **52,** 1150–1152 (1937).
10. V. R. Rao, *Ind. J. Phys.* **23,** 535 (1949).
11. E. A. Shenyavskaya, Y. Y. Kuzyakov, and V. M. Tatevskii, *Opt. Spectrosc.* **12,** 197–199 (1962).
12. A. Chatalic, P. Deschamps, and G. Pannetier, *C. R. Acad. Sci. Paris* **268,** 1111–1113 (1969).
13. R. L. Diebner and J. G. Kay, *J. Chem. Phys.* **51,** 3547–3554 (1969).
14. K. P. Lanini, Ph.D. dissertation, University of Michigan, Ann Arbor, MI, 1972.
15. T. C. DeVore, *High Temp. Sci.* **15,** 263–273 (1982).
16. J. G. Phillips and S. P. Davis, *Astrophys. J. Suppl. Ser.* **71,** 163–172 (1989).
17. T. Imajo, D. Wang, K. Tanaka, and T. Tanaka, Paper MG10, 53rd International Symposium on Molecular Spectroscopy, June 1998.
18. J. G. Phillips, S. P. Davis, and D. C. Galehouse, *Astrophys. J. Suppl. Ser.* **43,** 417–434 (1980).
19. R. B. Le Blanc, J. B. White, and P. F. Bernath, *J. Mol. Spectrosc.* **164,** 574–579 (1994).
20. J. Anglada, P. J. Bruna, and S. D. Peyerimhoff, Mol. Phys. **69,** 281–303 (1990).